

Determination of Chain Conformation of Stiff Polymers by Depolarized Rayleigh Scattering in Solution

G. Petekidis[†] and D. Vlassopoulos*

Foundation for Research & Technology–Hellas, Institute of Electronic Structure & Laser, P.O. Box 1527, Heraklion 71110, Crete, Greece

P. Galda, M. Rehahn, and M. Ballauff

Polymer-Institut der Universität Karlsruhe, Kaiserstrasse 12, 76128 Karlsruhe, Germany

Received July 29, 1996; Revised Manuscript Received October 15, 1996[®]

ABSTRACT: The chain conformation of a series of polydisperse polyesters and poly(*p*-phenylenes) has been investigated by means of depolarized Rayleigh scattering in solution. By considering polydisperse worm-like chains, using a Schultz–Zimm distribution, the persistence length, q , was determined from the specific depolarized Rayleigh ratio at infinite dilution and the weight average chain contour length, without involving optical anisotropies or the internal field problem. This general analysis showed that the effect of polymer nonuniformity is nearly negligible. For the polyester, q was found to be approximately 19 nm, whereas for the poly(*p*-phenylene) it was about 28 nm; these values exhibit the correct trend, but are higher than the corresponding ones from other techniques. Deviations are mainly attributed to the limited range of molecular weights available; this restricts the polyesters near the coil limit and the poly(*p*-phenylenes) near the rod limit. Using optical anisotropy data of the monomers and various oligomers, the validity of Flory's additivity scheme is verified for these systems.

I. Introduction

It is well-known that rigid-rod polymers are characterized by a large persistence length, which is a direct measure of the chain stiffness and is intimately related to the type and stability of the mesophases formed.¹ Accurate knowledge of this property is essential in understanding the mechanical behavior of the rigid-rod polymers, as well as the coupling between translation and rotation, and other features of the dynamic behavior near the isotropic to nematic transition.²

Several techniques have been used for the determination of the conformational properties of polymers and oligomers in solution. Among them are magnetic birefringence (Cotton–Mouton effect),³ polarized dynamic light scattering,⁴ viscosimetry (Bohdanecky method),⁵ electric birefringence (Kerr effect),⁶ flow birefringence,⁷ scattering by X-rays or neutrons,⁸ intrinsic dynamic viscoelastic moduli,⁹ whereas for very long biological polymeric filaments, fluorescence microscopy appears to be very effectively.¹⁰ Of special interest is the technique of depolarized Rayleigh scattering (DRS), which has been successfully utilized for the measurement of the optical anisotropy of low-molecular weight nematogenic compounds,¹¹ as well as polymeric systems.¹²

Recently, a general approach was presented, which relates magnetic birefringence measurements to the conformational properties of polydisperse polymers in solution;¹³ it accounts for the important characteristics of the polymers investigated, i.e. chain flexibility (worm-like) and polydispersity. The present investigation applies essentially the same general analysis of the conformation of semiflexible chains to the depolarized Rayleigh spectra from polymers of different stiffness. The technique used was Fabry–Perot interferometry (FPI), which produced spectra that were appropriately

analyzed in order to reveal the specific depolarized Rayleigh ratio at infinite dilution and eventually determine the persistence length. When compared to the polarized light scattering, DRS is more efficient in measuring low molecular weight samples as well. The reason is the fact that the depolarized intensity is related to

$$\sum_{i,j} \left| \frac{3 \cos^2 \theta_{ij} - 1}{2} \right|$$

for all elements i and j along the chain, and thus when applying the worm-like model, we are led to a quantity which varies in a very similar way to the radius of gyration, but with an apparent persistence length 3 times smaller.¹⁴

The paper is organized as follows: section II presents the analysis of DRS from semiflexible polydisperse polymer chains. The experimental procedure is outlined in section III, and the ultimate determination of the persistence length is discussed in section IV. Finally, section V summarizes the main findings and conclusions.

II. Depolarized Rayleigh Scattering from Semiflexible Polymer Chains

Depolarized Rayleigh scattering is already established as a reliable experimental technique for the measurement of the mean square optical anisotropy ($\langle \gamma^2 \rangle$) of nematogenic oligomeric compounds.¹¹ The scattering of laser light in the depolarized mode (VH) is induced by orientation fluctuations, which cause fluctuation of the anisotropic part of the polarizability tensor. In addition to the intrinsic molecular anisotropy, the collision-induced anisotropy contributes to the total depolarized Rayleigh intensity. For a system of symmetric top molecules, the integrated depolarized intensity at zero scattering wavevector is given by¹¹

* Author to whom correspondence should be addressed.

[†] Also in the Department of Physics, University of Crete, Heraklion 71110, Crete, Greece.

[®] Abstract published in *Advance ACS Abstracts*, December 15, 1996.

$$I_{\text{VH}} = A f(n) \frac{1}{n^2} \rho \langle \gamma^2 \rangle (1 + \rho F_c) + I_{\text{CI}} \quad (1)$$

where A is a constant, $f(n)$ is the local field correction, $1/n^2$ is a geometrical factor (n being the refractive index of the medium), ρ is the number density of the anisotropic scatterers, $\langle \gamma^2 \rangle$ is the mean square optical anisotropy (averaged over all possible molecular conformations), and I_{CI} is the collision-induced contribution to the scattering intensity. The term $(1 + \rho F_c)$ represents the intermolecular interactions, directly connected with the fluid structure; F_c is a measure of the orientational pair correlations, which is concentration-dependent (when no orientational correlation exists, $F_c = 0$). The molecular optical anisotropy is defined from the traceless part of the polarizability tensor, \mathbf{a}_0 , by

$$\gamma^2 = \frac{3}{2} \text{trace}(\hat{\mathbf{a}}_0 \hat{\mathbf{a}}_0) \quad \text{with} \quad \hat{\mathbf{a}}_0 = \mathbf{a}_0 - \frac{1}{3} \text{trace}(\mathbf{a}_0) \mathbf{E} \quad (2)$$

where $\mathbf{E} = \text{diag}(1, 1, 1)$. If we further consider cylindrical symmetry around the main axis x of the molecule, then

$$\gamma^2 = (\Delta \mathbf{a}_0)^2 + \frac{3}{4} (\Delta \mathbf{a}_0^+)^2 \quad (3)$$

with $\Delta \mathbf{a}_0 = a_{xx} - (a_{yy} + a_{zz})/2$ being the cylindrical term, and $\Delta \mathbf{a}_0^+ = a_{yy} - a_{zz}$ the acylindrical term, in which $\hat{\mathbf{a}}_0$ decomposes

$$\hat{\mathbf{a}}_0 = \Delta \mathbf{a}_0 J + \Delta \mathbf{a}_0^+ J^+ \quad (4)$$

where $J = \text{diag}(2/3, -1/3, -1/3)$ and $J^+ = \text{diag}(0, 1/2, -1/2)$. In order to deduce the molecular contribution to the depolarized intensity (or the intrinsic molecular anisotropy $\langle \gamma^2 \rangle$, directly connected with it), the contribution of the collision-induced anisotropy, I_{CI} , should be subtracted from the measured I_{VH} . The characteristic time associated with the collisions between solvent molecules or solvent and polymer molecules is much smaller than the reorientational time of both solvent molecules and polymer molecules; this allows a clear distinction between the two relevant dynamic processes in a DRS experiment.

Concerning the internal field problem (IFP), which is still open in DRS, we used the second power correction, which has been demonstrated experimentally to work reasonably well.^{11,12,13,15} Thus,

$$f(n) = \left(\frac{n^2 + 2}{3} \right)^2$$

which is consistent with the use of Flory's additivity approximation,¹⁶ which is actually the additivity of the bond polarizability tensor, as well. Whereas a rigorous approach apparently favors the fourth-power correction,¹⁷ the choice of the appropriate power can be essentially bypassed in the actual analysis of chain conformation from DRS, as discussed below.

For the determination of the optical anisotropy, we assume that the molecule consists of symmetric top repeating units, each having anisotropy $\langle \gamma_0^2 \rangle$. Furthermore, by assuming the applicability of Flory's group additivity approximation, and by utilizing the worm-like model prediction for

$$\langle \gamma^2 \rangle = \langle \gamma_0^2 \rangle \sum_{ij} \frac{3 \langle \cos^2 \theta_{ij} \rangle - 1}{2}$$

with θ_{ij} the angle between the axes of the optical ellipsoids associated with segments i and j , the following estimation of the polymer's average optical anisotropy is obtained¹⁴ (where only the cylindrical terms are taken into account):

$$\langle \gamma^2 \rangle = \langle \gamma_0^2 \rangle q F(L) \left(\frac{2}{3} \frac{N}{l_0} \right) \quad (5)$$

where q is the persistence length and l_0 the contour length of the repeating unit, L the contour length, and N the number of monomers in the chain, and $F(L)$ is given by

$$F(L) = \left(1 - \frac{q}{3L} [1 - e^{-3L/q}] \right) \quad (6)$$

In the limit of zero concentration, the depolarized intensity due to the intrinsic anisotropy is proportional to the average molecular anisotropy of the polymer:

$$\left(\frac{R_{\text{VH}}}{\rho} \right)_{\rho \rightarrow 0} = \frac{1}{15} \left(\frac{2\pi}{\lambda} \right)^4 \left(\frac{n^2 + 2}{3} \right)^2 \langle \gamma^2 \rangle \quad (7)$$

with

$$R_{\text{VH}} = \left(\frac{I_{\text{VH}}}{I_{\text{tol}}} \right) \left(\frac{n}{n_{\text{tol}}} \right)^2 R_{\text{VH,tol}}$$

being the contribution of the polymer to the VH scattering. $R_{\text{VH,tol}}$ is the depolarization ratio of toluene, which was used as reference in this work; λ is the wavelength of the laser light. It is now straightforward from the above analysis to use eq 7 in order to deduce an expression for the depolarization ratio at infinite dilution (normalized by the weight concentration, c , in g/cm³), which is the quantity directly measured with the DRS technique:

$$\left(\frac{R_{\text{VH}}}{c} \right)_{c \rightarrow 0} = K_{\text{DRS}} q F(L) \quad (8)$$

where K_{DRS} is a constant associated with the DRS technique, given by

$$K_{\text{DRS}} = \left(\frac{2\pi}{\lambda} \right)^4 \left(\frac{n^2 + 2}{3} \right)^2 \frac{2}{45} \frac{N_A}{l_0 M_0} \langle \gamma_0^2 \rangle \quad (9)$$

where N_A is the Avogadro number and M_0 the molecular weight of the repeating unit.

When accounting for the effects of polydispersity, the quantitative treatment of the DRS data follows essentially the magnetic birefringence data analysis;¹³ actually, the basic physics behind the two techniques is the same, and both treatments converge to the same scaling predictions. It is noted that, when dealing with the light scattering intensity R_{VH} , we have to weight the contributions of the respective species of a nonuniform polymer with their weight fraction. This follows from the fact that eq 8 also can be written as $R_{\text{VH}} = (K_{\text{DRS}}/N_A) M \rho F(L) q$ and for polydisperse samples as $R_{\text{VH}} \sim \int M \rho(M) F(M) dM = \int L \rho(L) F(L) dL = \int w(L) F(L) dL$, where $\rho(M)$ is the number fraction of species with mass M and $w(L)$ the weight fraction of species of length L (contour length distribution). Hence, in the generalized

analysis of the DRS data for nonuniform polymers, the specific depolarized light intensity can be written as

$$\left[\frac{R_{\text{VH}}}{c} \right]_{c \rightarrow 0} = K_{\text{DRS}} q \int_0^\infty w(L) F(L) dL \quad (10)$$

By using the Schultz-Zimm distribution,

$$w(L) = y^{m+1} \frac{L^m}{m!} \exp(-yL) \quad (11)$$

where $y = (m + 1)/L_w$, $m = (L_w/L_n - 1)^{-1}$ is the polydispersity index, and L_w and L_n are the weight and number average contour lengths, respectively. The integration of eq 10 leads to

$$\left[\frac{R_{\text{VH}}}{c} \right]_{c \rightarrow 0} = K_{\text{DRS}} q \left[1 - \frac{m+1}{m x_w} \left(1 - \left(1 + \frac{x_w}{m+1} \right)^{-m} \right) \right] \quad (12)$$

where $x_w = 3L_w/q$ is the reduced contour length. The two limiting cases of interest are the high and the low molecular weights, corresponding to the coil and rod limits, respectively:

$$(i) \ x_w \gg 1: \quad \frac{R_{\text{VH}}}{c} \rightarrow K_{\text{DRS}} q \quad (13)$$

$$(ii) \ x_w \ll 1: \quad \frac{R_{\text{VH}}}{c} \rightarrow \frac{3}{2} K_{\text{DRS}} L_w \quad (14)$$

As in the Cotton–Mouton case, this result suggests that, in both limits, the depolarized light scattering intensity (and thus the average optical anisotropy) is independent of the width of the molecular weight distribution. Additionally, for very long chains, it is also independent of molecular weight (coil-like behavior), while for short chains, it is directly proportional to L_w (rigid-rod-like behavior). It is easy to show from eq 12 that in the intermediate region the influence of the polydispersity index m is rather limited. Thus, by using in general the most probable distribution ($m = 1$), we end-up with:

$$\frac{K_{\text{DRS}} q}{[R_{\text{VH}}/c]_{c \rightarrow 0}} = 1 + \frac{2}{x_w} \quad (15)$$

Equation 15 suggests that it is possible to determine the persistence length of a polydisperse polymer by simply plotting dR_{VH}/dc (at $c \rightarrow 0$) against $1/L_w$. Thus, the persistence length can be determined from DRS without invoking the IFP (which is incorporated into K_{DRS}). Further, the effect of the typically high polymer non-uniformity turns out to be nearly insignificant.

III. Experimental Section

Materials. The polyester TPPE (shown in Chart 1, together with its trimer, a 2',5'-di-*n*-hexyl-*p*-terphenyl-4,4''-diol) and the poly(*p*-phenylene) PPP (shown in Chart 2, together with its oligomers) used in this work, were synthesized by polycondensation. A range of molecular weights M_w from 11 300 to 130 000 and from 31 680 to 47 850 were obtained for the TPPE and the PPP, respectively. Details for the TPPE and PPP synthesis can be found elsewhere.^{18,19} The solvent used in this study was HPLC-grade chloroform, and dust-free samples were obtained by filtration through a 0.22- μm Teflon Millipore filter directly into the dust-free light scattering cells ($1 \times 1 \times 4$ cm rectangular cells from Hellma). The DRS measurements were carried out at concentrations ranging from 0.03% per weight to 4.4% per weight. The upper bound was determined by the

Chart 1. Polyester TPPE with hexyl side chains and its trimer

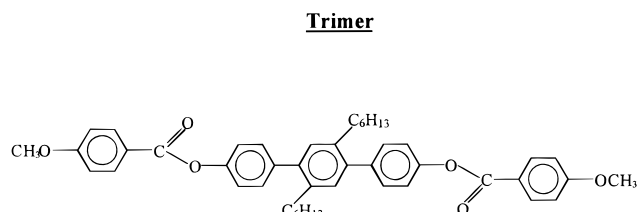
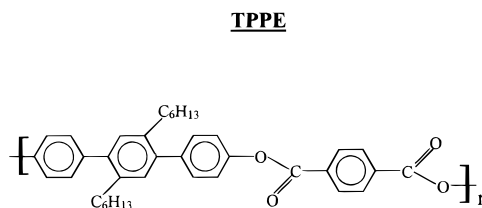


Chart 2. Poly(*p*-phenylene) PPP with dodecyl side chains and its oligomers 2:0 (no side chains), 3:0 (no side chains), 3:6 (hexyl side chains), and 3:12 (dodecyl side chains)

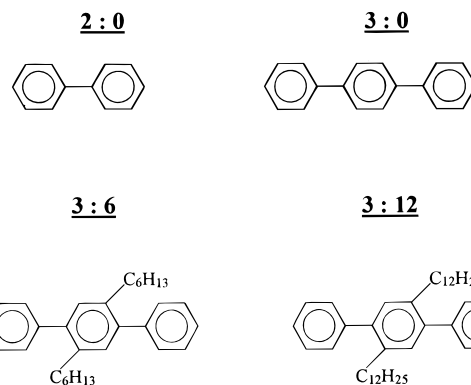
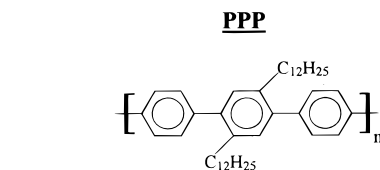


Table 1. Molecular and Optical Characteristics of the Polyester TPPE Series and the Trimer

sample	M_w	L_w (nm)	m^a	$R_{\text{VH}}/c \times 10^6$ (cm^2/g)	$\langle \gamma^2 \rangle / N$ (\AA^6)
trimer	699	3.0	∞	62	1601 ($N = 1$)
TPPE-1	11300	44.4	(1.67) ^b	205	5597
TPPE-2	20400	80.2	1.43	224	6115
TPPE-3	31100	122	1.67	249	6798
TPPE-4	47200	185	1.11	251	6853
TPPE-5	130000	511	0.48	256	6990

^a Polydispersity index: $m = (L_w/L_n - 1)^{-1}$. ^b The value in parentheses is an estimation based on the m 's and L_w 's of the other polymers of the series.

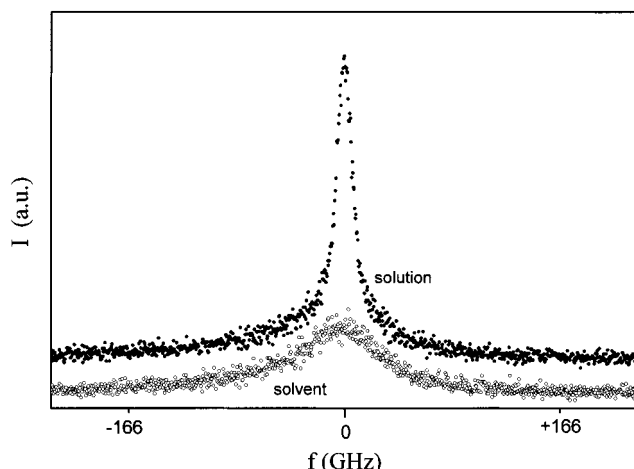
solubility of each sample.²⁰ Molecular and optical characteristics of the various TPPE polyesters and trimer are shown in Table 1, whereas those of the various PPP poly(*p*-phenylenes) and oligomers are in Table 2. The biphenyl (2:0) and terphenyl (3:0) samples were obtained from Aldrich.

Apparatus and Measurements. A detailed description of the experimental system used has been presented else-

Table 2. Molecular and Optical Characteristics of the Poly(*p*-phenylene) PPP-12 Series and the Oligomers 2:0, 3:0, 3:6, and 3:12

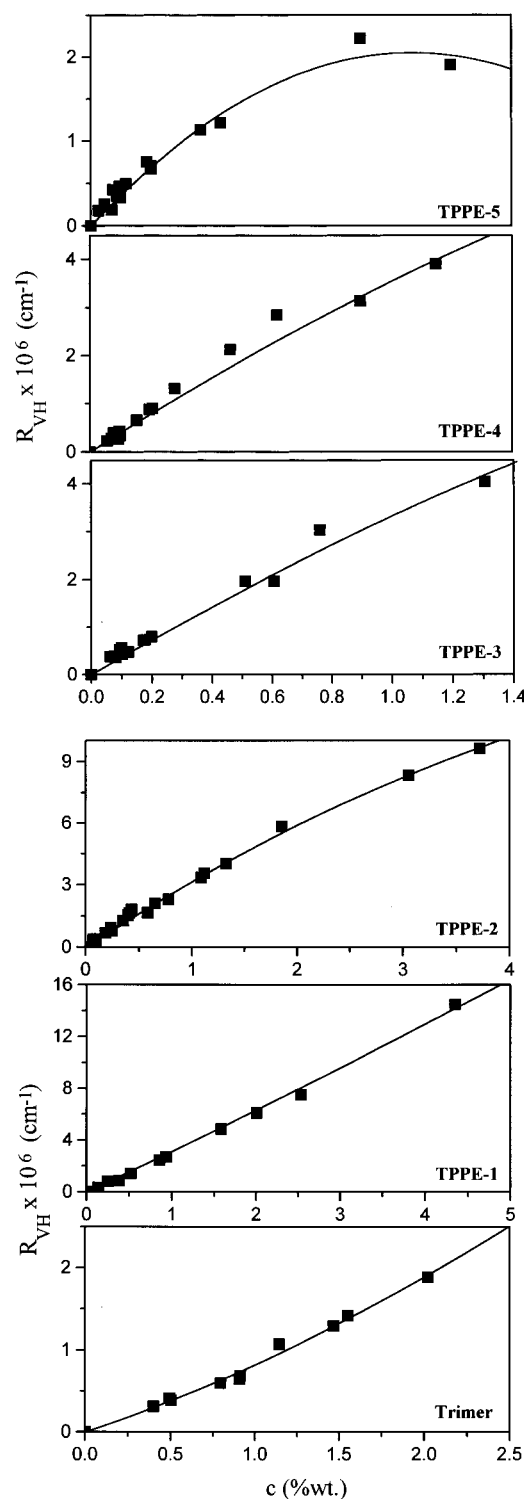
sample	M_w	L_w (nm)	m^a	$R_{VH}/c \times 10^6$ (cm ² /g)	$\langle \gamma^2 \rangle / N$ (Å ⁶)
2:0	154	0.84	∞	24.64	185 ($N=1$)
3:0	230	1.33	∞	45.23	529 ($N=1$)
3:6	398	1.33	∞	16.5	319 ($N=1$)
3:12	566	1.33	∞	16	441 ($N=1$)
PPP monomer	564	1.48	∞	24.9	686 ($N=1$)
PPP-1	31680	82.2	(0.45) ^b	241	6650
PPP-2	39060	101.1	0.48	308	8499
PPP-3	43200	117.2	0.45	307	8472
PPP-4	47850	123.2	0.43	342	9438

^a Polydispersity index: $m = (L_w/L_n - 1)^{-1}$. ^b The value in parentheses is an estimation based on the m 's and L_w 's of the other polymers of the series.

**Figure 1.** Typical depolarized Rayleigh spectrum of a polyester TPPE-3 solution in chloroform (0.1% by weight), at a scattering angle of 90°, and the corresponding spectrum of the solvent.

where.¹¹ Briefly, the light source used was an argon ion laser (Spectra Physics Model 2020), operating at 488 nm with stabilized power of 300 mW. The spectrum of the scattered, at 90° angle, depolarized light (a typical example is depicted in Figure 1) was taken using a planar Fabry-Perot interferometer (Spectra Physics Model 381) with a free spectral range of 983 GHz (40 cm⁻¹); the sample was stabilized at a temperature of 25 °C. In the depolarized geometry, the incident beam is polarized vertical and the scattered horizontal, relative to the scattering plane, by using Glan-Thomson polarizers (extinction coefficients 10⁻⁶ and 10⁻⁷, respectively).

The accurate and reproducible measurement of I_{VH} required proper consideration of the important factors already mentioned above, namely the I_{Cl} , F_c , and the dependence on the wavevector q . The utilization of a Fabry-Perot interferometer enables us to subtract the contribution of I_{Cl} , since it appears as a broad background in the Rayleigh spectrum dominated by the Rayleigh peak due to the significantly slower molecular reorientation. The obtained intensity spectrum $I_{VH}(\omega)$ was integrated in order to get the actual intensity I_{VH} . Figure 1 depicts a typical depolarized Rayleigh spectrum for the polymer solution and solvent (TPPE-3 in chloroform, concentration 0.1% by weight), along with the corresponding spectrum from pure chloroform. The VH component of the scattered intensity of the polymer can be isolated from the solvent background and calculated from $I_{\text{solute}} = I_{\text{solution}} - (1 - \phi)I_{\text{solvent}}$, ϕ being the percent concentration of the solute. Further, the q -independence of the intensity I_{VH} was always preserved; this guaranteed the validity of eq 1 above. Finally, in order to avoid intermolecular interactions, the specific depolarization ratio R_{VH}/c was determined at the infinite dilution limit, using $R_{VH}(\text{tol}) = 4.88 \times 10^{-6}$ cm⁻¹.¹¹ To accomplish this, it was necessary to undertake numerous

**Figure 2.** Depolarized Rayleigh ratio of the polyester TPPE samples (TPPE-1, TPPE-2, TPPE-3, TPPE-4, and TPPE-5) and the trimer, as a function of concentration, and corresponding nonlinear fits.

careful measurements in a wide range of concentrations, as discussed below.

IV. Results and Discussion

Since the analysis presented above is valid for negligible molecular interactions, and even at low concentrations our data exhibit a clear deviation from linearity, we used a nonlinear fitting procedure in order to extract the limiting value of dR_{VH} at $c \rightarrow 0$. Figure 2 shows the depolarized Rayleigh ratio as a function of concen-

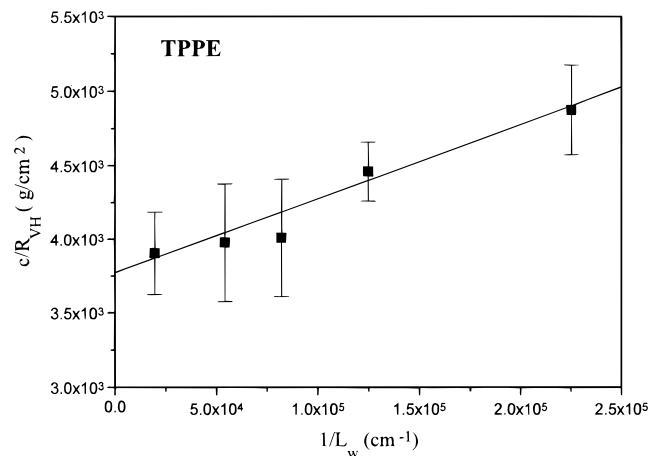


Figure 3. Determination of the persistence length of the polyester TPPE, using the linear equation 15, expressing $(c/R_{VH})_{c \rightarrow 0}$ as a function of L_w^{-1} . The solid line represents the least-squares fit.

tration for all five TPPE polyester samples and the trimer. It is clear that, as the concentration increases, molecular interactions come into play. A reasonably good nonlinear fitting is obtained for all samples; it should be noted, however, that the slope at vanishing concentration, $(R_{VH}/c)_{c \rightarrow 0}$, differs only slightly from sample to sample, and this is explained by the fact that due to the limited range of molecular weights used, there was not much difference in scattering power from the low to the high molecular weight. A closer look at the data, however, reveals an additional interesting feature: as the molecular weight increases, the second derivative of R_{VH} versus c changes sign. To explain this behavior, we argue that short chains (trimer and maybe TPPE-1) are near the rod limit, whereas the longer chains (TPPE-2, TPPE-3, TPPE-4, and TPPE-5) are near the coil limit. Thus, we expect that in the former case intermolecular interactions dominate at relatively high concentrations, while in the latter one intramolecular interactions might be also involved; these interactions may lead to a slight change in the average segmental pair orientation, expressed by the second Legendre polynomial, from positive (average orientation angle below 55°) to negative (average orientation angle above 55°), which eventually results to the observed change in curvature. Negative curvatures have been reported in the past, with flexible polymers.^{12,21,22} In the case of the poly(*p*-phenylene) series, the concentrations used were below 1.2% by weight, and thus the R_{VH} versus c plots were linear, for all samples PPP-1, PPP-2, PPP-3, and PPP-4, with reasonably good statistics.

Figures 3 and 4 represent the use of eq 15 in order to determine the average conformation of the polyester and poly(*p*-phenylene) chains. First of all, it is also noted that the approximate value of m for the polymers investigated in this work varies from 0.4 to 1.7, as determined by GPC (Tables 1 and 2). Using this information, it is easy to calculate the relative errors from applying eq 15 to polyesters and poly(*p*-phenylenes). For the polyester samples TPPE-5, TPPE-4, TPPE-3, TPPE-2, and TPPE-1, the maximum error ranges from 1% to 6%. For the poly(*p*-phenylene) samples PPP-1, PPP-2, PPP-3, and PPP-4, with an average $m = 0.45$, the calculated error is around 5%. The least squares line fits the experimental data, with some uncertainty, but given the difficulties and limitations, we argue that Figures 3 and 4 demonstrate the applicability of eq 15 in determining the persistence

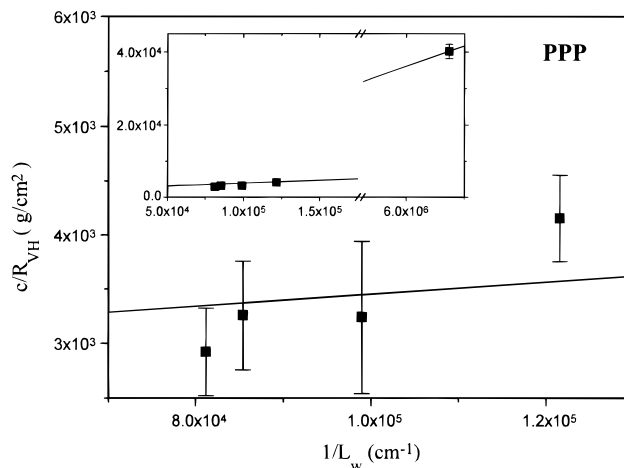


Figure 4. Determination of the persistence length of the poly(*p*-phenylene) PPP, from the developed linear equation 15, expressing $(c/R_{VH})_{c \rightarrow 0}$ as a function of L_w^{-1} . For clarity, only the four PPP data points are presented, whereas the monomer is included in the inset which demonstrates the importance of having a wide range of molecular weights available. Solid lines represent the least-squares fit (notice the scale of L_w^{-1}).

length of a stiff polymer. The result from the slope and intercept of Figure 3 is approximately $q = 19$ nm. Furthermore, from the intercept, the value of the DRS constant was determined as $K_{DRS} = 133 \pm 20$ cm/g. This value of q is clearly higher than the corresponding values on the same polyester, measured with different techniques (11.0 nm with magnetic birefringence¹³ and 9.0–11.0 nm with viscosimetry¹⁸). It should be noted that the difference in the values of the persistence lengths obtained from different techniques, reported in the literature, is usually high, much higher than the ones reported here.^{9,12} A wider range of molecular weights would lead to a more certain best fit line, and thus q . This is especially true for low molecular weights, as concluded from Figure 3 (where actually all data points but one are in the coil limit).

As already mentioned, the use of the worm-like model in the calculation of the optical anisotropy is based on the validity of the additivity of the monomer anisotropy. Hence, it is imperative to check this assumption by utilizing K_{DRS} from eq 15. For TPPE, by using eq 9 and the value of K_{DRS} determined experimentally, as well as $l_0 = 22$ Å, $m_0 = 560$, and $f(n) = 1.859$, the effective optical anisotropy of the monomer was estimated to be 1196 ± 180 Å⁶. By considering only the cylindrical contribution to the optical anisotropy ($\langle \gamma^2 \rangle \approx \Delta \alpha^2$), the measured $\Delta \alpha$ of the monomer is 34.6 ± 2.5 Å³, whereas the calculated one is 32 Å³, corresponding to a relative error of 8%. This calculation was based on the experimentally determined value of $\langle \gamma_0^2 \rangle$ of the oligomer 3:6 (from the measured R_{VH}/c), which amounts to 319 Å⁶ ($\Delta \alpha = 17.86$ Å³), and on the use of Flory's additivity scheme, based on the measured optical anisotropy of various groups composing the trimer. These are as follows:^{12,14} $\Delta \alpha(\text{OCH}_3) = 0.072$ Å³, $\Delta \alpha(\text{phenyl}) = 7.97$ Å³, $\Delta \alpha(\text{OCO}) = 1.02$ Å³, and a change of the $\Delta \alpha$ of the phenyls in the 3:6, when they are substituted in the trimer (0.097 Å³). In addition to the above, the trimer was directly measured, yielding a value of $\langle \gamma^2 \rangle = 1601$ Å⁶ (Table 1), and thus $\Delta \alpha = 40.01$ Å³, whereas the estimated anisotropy according to Flory's group additivity scheme, based on the above values for various groups, is $\Delta \alpha = 37.92$ Å³. This corresponds to a small relative error of 5%. These results, the direct measurement of the trimer anisotropy and the measurement of

monomer anisotropy deduced from the DRS analysis of the polydisperse polymer, confirm the validity of the Flory's incremental scheme, with a small error. Further, they support the physical basis for the use of the worm-like model to account for the conformation of such stiff polymers.

The persistence length of the PPP poly(*p*-phenylene) series was determined to be approximately 28 nm, whereas K_{DRS} was found to be 120 cm/g, with similar remarks concerning experimental uncertainty as in the TPPE case. As seen in Figure 4, the monomer 3:12 was also used for extracting this value, based on the validity of Flory's incremental scheme discussed above; further it served as the low molecular weight limit (all samples appeared to be in the rod limit anyway; thus, the q determined was a low bound). It is noted that the value of the specific depolarization ratio for the monomer used in Figure 4 was determined from the measurements of the oligomer 3:12 by adding the contribution of substituted phenyls at the ends; the latter is estimated from the 2:0 and 3:0 oligomers. The result is $R_{\text{VH}}/c = 24.9 \times 10^{-6} \text{ cm}^2/\text{g}$. The above results indicate that PPP is a stiffer polymer than TPPE; this is considered reasonable, since due to the differences in the chemical structure of these polymers, as revealed in Charts 1 and 2, in the PPP case the phenyl groups are directly connected in the polymer backbone, resulting in a stiffer molecule. It should also be mentioned that recent computer simulations with such materials (PPP) confirm their large stiffness (compared to polyesters), predicting a persistence length of about 22.0 nm.²³

V. Conclusions

A general method has been presented for the analysis of the average conformation of stiff polymer chains, by using depolarized Rayleigh scattering data in solution. It invokes the worm-like chain model and accounts for the polymer polydispersity. The persistence length, q , is determined by a simple universal plot of the reciprocal of the specific depolarization ratio versus the reciprocal of the weight average chain length. Results for the polyester series TPPE ($q = 19 \text{ nm}$) and the poly(*p*-phenylene) series PPP ($q = 28 \text{ nm}$) confirm that poly(*p*-phenylenes) are stiffer molecules than polyesters, but are higher than the ones obtained with different techniques, due to the errors associated with the limited range of molecular weights available. Finally, by determining the effective anisotropy of oligomers, using the second-power correction to the internal field, and comparing against the calculated values of the substituent units, it is shown that Flory's group additivity approximation works well for these systems.

Acknowledgment. The financial support of the European Community (grant BE-4490-90) and the

Greek General Secretariat for Research and Technology (GSRT-Basic Research) is gratefully acknowledged. G.P. and D.V. would like to further acknowledge helpful discussions with Professor G. Fytas.

References and Notes

- (1) Ballauff, M. In *Materials Science and Technology*; Cahn, R. W.; Haasen, P.; Kramer, E. J., Eds.; VCH: Weinheim, 1993. Ballauff, M. *Angew. Chem.* **1989**, *28*, 253. Wissbrun, K. F. *J. Rheol.* **1981**, *25*, 619.
- (2) Russo, S. P. In *Dynamic Light Scattering: The Technique and Some Applications*; Brown, W., Ed.; Oxford Science Publications: Oxford, UK, 1993; Tracy, M. A.; Pecora, R. *Annu. Rev. Phys. Chem.* **1992**, *43*, 525. Petekidis, G.; Fytas, G.; Witteler, H. *Colloid Polym. Sci.* **1994**, *272*, 1457.
- (3) Fraden, S.; Maret, G.; Caspar, D. L. D. *Phys. Rev. E* **1993**, *48*, 2816. Fuhrmann, K.; Martin, A.; Maret, G.; Tiesler, U.; Ballauff, M. *J. Phys. Chem.* **1994**, *98*, 4094.
- (4) Coviello, T.; Kajiwar, K.; Burchard, W.; Dentini, M.; Crescenzi, V. *Macromolecules* **1986**, *19*, 2826. Sato, R.; Norisuye, T.; Fujita, H. *Macromolecules* **1984**, *17*, 2696.
- (5) Bohdanecky, M. *Macromolecules* **1983**, *16*, 1483.
- (6) Watanabe, H.; Yoshioka, K. *Biopolymers* **1966**, *4*, 43.
- (7) Tsvetkov, V. N.; Andreeva, L. N. *Adv. Polym. Sci.* **1981**, *39*, 95.
- (8) Kirste, R. G.; Oberthur, R. C. In *Small Angle X-ray Scattering*; Glatter, O.; Kratky, O., Eds.; Academic Press: London, 1982.
- (9) Carriere, C. J.; Amis, E. J.; Schrag, J. L.; Ferry, J. D. *J. Rheol.* **1993**, *37*, 469.
- (10) Ott, A.; Magnasco, M.; Simon, A.; Libcharber, A. *Phys. Rev. E* **1993**, *48*, R1642.
- (11) Fytas, G.; Patkowski, A. In *Dynamic Light Scattering: The Technique and Some Applications*; Brown, W., Ed.; Oxford: UK, 1993; Floudas, G.; Patkowski, A.; Fytas, G.; Ballauff, M. *J. Phys. Chem.* **1990**, *94*, 3215.
- (12) Takaeda, Y.; Yoshizaki, T.; Yamakawa, H. *Macromolecules* **1993**, *26*, 3742.
- (13) Tiesler, U.; Rehahn, M.; Ballauff, M.; Petekidis, G.; Vlassopoulos, D.; Maret, G.; Kramer, H. *Macromolecules* **1996**, *29*, 6832.
- (14) Arpin, M.; Strazielle, C.; Weill, G.; Benoit, H. *Polymer* **1977**, *18*, 262.
- (15) Irvine, P. A.; Erman, B.; Flory, P. J. *J. Phys. Chem.* **1983**, *87*, 2929.
- (16) Flory, P. J. *Statistical Mechanics of Chain Molecules*, 2nd ed.; Hanser Publishers: München, 1989.
- (17) Keyes, T.; Ladanyi, B. M. *Adv. Chem. Phys.* **1986**, *56*, 411.
- (18) Tiesler, U.; Pulina, T.; Rehahn, M.; Ballauff, M. *Mol. Cryst. Liq. Cryst.* **1994**, *243*, 299. Kallitsis, J. K.; Wegner, G.; Pakula, T. *Makromol. Chem.* **1992**, *193*, 1031.
- (19) Galda, P. *Ph.D. Thesis*, Karlsruhe, 1993. Rehahn, M.; Schlüter, A.-D.; Wegner, G. *Makromol. Chem.* **1990**, *191*, 1991. Galda, P.; Rehahn, M. *Synthesis* **1996**, 614.
- (20) Petekidis, G.; Vlassopoulos, D.; Fytas, G.; Kountourakis, N.; Kumar, S. *Macromolecules* **1996**, submitted.
- (21) Lin, Y.-H.; Fytas, G.; Chu, B. *J. Chem. Phys.* **1981**, *75*, 2091. Takaeda, Y.; Yoshizaki, T.; Yamakawa, H. *Macromolecules* **1993**, *26*, 3742.
- (22) Konishi, T.; Yoshizaki, T.; Shimada, J.; Yamakawa, H. *Macromolecules* **1989**, *22*, 1921.
- (23) Farmer, B. L.; Chapman, B. R.; Dubis, D. S.; Adams, W. W. *Polymer* **1993**, *34*, 1588.

MA961128X